Acta Geotechnica
https://doi.org/10.1007/s11440-024-02294-z

RESEARCH PAPER

Controllable hydrophobization of sands with self-healing polymeric microcapsules

Rui Qi[1] · Ke Chen[1] · Hongjie Lin[2] · Sérgio D. N. Lourenço[1] · Antonios Kanellopoulos[3]

Received: 9 March 2022 / Accepted: 14 February 2024

Abstract
Hydrophobized soils have functional hydrophobic coatings to delay or restrict water infiltration and thus prevent infrastructure failure and long-term degradation. Over time, hydrophobized soils will be subjected to degradation under the action of external stresses, leading to the loss of its functional properties. Microencapsulation approaches, initially developed for self-healing applications emerge as a potential solution to enhance, switch (from hydrophilic) or prolong the longevity of hydrophobized soils. The aim of this study is to produce and investigate the effectiveness of microencapsulation to impart hydrophobicity in granular materials in response to external stimuli. In this research, polydimethylsiloxane (PDMS), with hydrophobic properties, is encapsulated in calcium alginate microcapsules with the ionic gelation method. The effectiveness of the microcapsules to induce hydrophobicity is investigated by mixing sand with microcapsules and quantifying the change of the contact angle and water drop penetration time (measures of hydrophobicity) under an external trigger, i.e., under drying and consecutive wetting–drying cycles. The results show that microcapsules release the hydrophobic cargo (PDMS) during shrinkage. After drying, the PDMS content in sand increased to 0.1–0.8% by mass of sand. The released hydrophobic cargo (PDMS) induced hydrophobicity in sands, reflected by a contact angle increase from 29.7° to at least 87.7°. The amount of polydimethylsiloxane encapsulated is a key parameter controlling the release of hydrophobic cargo. In addition, 4% capsule content in sands is identified as an effective microcapsule content in inducing hydrophobicity.

Keywords Calcium alginate · Hydrophobicity · Microcapsules · Polydimethylsiloxane · Release behavior · Sands

1 Introduction

The aging of infrastructure through the degradation of materials is expected to have profound impacts on its lifespan. Degradation of materials can be driven by physical factors (e.g., increased erosion in embankments due to extreme weather events), chemical factors (e.g., weathering) and biological factors (e.g.,, biofilms) [48]. Hydrophobized soils are initially hydrophilic, whose particles have been functionalized to acquire hydrophobic properties, allowing their use in ground infrastructure to delay or restrict water infiltration. In general, they can find application as interface materials with the atmosphere or buried in the ground in contact with structures and have been tested as a protection layer for slopes to restrict water infiltration, cover layer for landfills, and protection surface for horse racing tracks [6, 22, 57]. Hydrophobized soils can be prepared by mixing soil with hydrophobic polymers such as dimethyldichlorosilane (DMDCS) and other silanes, polydimethylsiloxane (PDMS), or fatty acids such as Tung oil [36]. However, hydrophobicity being a surface property is unlikely to last the lifespan of an engineering structure. The level of hydrophobicity will eventually decline, and their surfaces revert to the original, that is

✉ Sérgio D. N. Lourenço
lourenco@hku.hk

[1] Department of Civil Engineering, The University of Hong Kong, Hong Kong, S.A.R., China

[2] Department of Civil Engineering, Sun-Yat Sen University, Guangzhou, China

[3] School of Physics, Engineering and Computer Science, Center for Engineering Research, University of Hertfordshire, Hertfordshire, UK

Published online: 18 May 2024

hydrophilic state. Previous studies reported the degradation of soil hydrophobicity due to physical abrasion where the hydrophobic coatings are chipped off exposing the underlying hydrophilic surfaces [34]. In addition, the hydrophobic films covering particles can undergo molecular changes due to temperature and humidity fluctuations, UV radiation and microorganisms. Therefore, there is a need to devise methods that could enhance the resistance of hydrophobic soils against adverse environmental factors and prolong their longevity.

In the last 10 years there has been a growing interest in applying self-healing materials to repair the damage of structures and to recover the performance of degraded materials [7, 31, 44]. Self-healing materials can fully or partially recover a functionality that occurs under service [7]. Concrete and asphalt have attracted most of the self-healing research in the construction materials domain. Typical self-healing systems include microcapsules, hollow fibers, among others [9, 58]. Microcapsules can store healing agents (or cargo) and protect them from an adverse environment, such as UV radiation, oxidation, or acids. The healing mechanism is based on the release of the stored healing agents triggered by an external stimulus. For microcapsules mixed with concrete, the healing process follows the rupture of microcapsules by fissures which releases healants, leading to precipitation and proliferation of crystalline products filling the fissures [30, 31, 52]. This results in healing of the cracks and recovery of properties such as permeability and strength. In surface coatings, microcapsules are also incorporated in the polymer coating matrix and provides the self-healing effect by releasing repairing agents due to crack propagation [44]. More recently, a microcapsules-based self-healing material has been applied to cemented soils. The mechanism is similar to that of cementitious materials. Microcapsules with epoxy resin cargo were mixed with cemented coral sand. During the damage process of the cemented soil sample, the microcapsules were ruptured, and the released epoxy resin cargo increased the soil strength by approximately 85% (3% of microcapsules by weight) [53]. Microcapsules with sodium silicate cargo have also been used in cemented soil for cutoff walls. The microcapsules were ruptured by the compressive loading and the released sodium silicate cargo improved the soil mechanical properties. The post-healing specimens regained 44% of their initial compressive strength [11]. Other releasing mechanisms relevant to soils, are based on the migration of cargo from inside to outside the microcapsules, the case of antioxidants release from microcapsules [26] or, the controlled release of nutrition (organic acids) in agriculture [12, 50]. Therefore, releasing hydrophobic cargo from microcapsules to increase soil hydrophobicity emerges as a potential solution to prolong the longevity of hydrophobized soils without the need to replace them.

Various encapsulation methods have been developed to be used in cementitious materials [31]. Pan coating (a physical method) has been used to encapsulate healing particles (nutrients and bacterial spores) with a geopolymer coating for healing microcracks in concrete [18]. Spray-drying (also physical) generates microcapsules by atomizing liquids in a hot gas while hardening the outer shell to sequester the core material [24] but its use is limited to heat-sensitive materials [8, 19]. The most common chemical encapsulation method is in-situ polymerization, whereby microcapsules with urea–formaldehyde shell and epoxy resin core are used as self-healing compounds in concrete [20, 23, 54] and cemented coral sand [55]. Physicochemical methods include ionic gelation and complex coacervation. Complex coacervation forms shells by means of ionic interactions between polymers [49]. For the ionic gelation method, the commonly used shell material is sodium alginate where calcium ions cross-link the alginate chains to form the microcapsules' shell made of calcium alginate. For complex coacervation, crosslinking occurs between two or more oppositely charged polymers, usually proteins and polysaccharides. Physicochemical methods are widely used in the food industry [10, 26], pharmaceuticals [26] and agriculture [50] and more recently, have been used to encapsulate bacteria [53] and sodium silicate [31] for self-healing concrete.

Previous studies in medicine and agriculture have shown that it is feasible to control the release of cargo from microcapsules under an external environmental action (pH or temperature change, wetting from liquid or water vapor) [4, 21, 40]. For controllable hydrophobization of sand by microcapsules, it is preferable the cargo releases by permeating through the shell, rather than by breakage due to tension or compression. This is because the target material in this study, sands, are volumetrically stable as they degrade. Based on this, calcium alginate microcapsules emerge as a suitable candidate to be used in sands. Calcium alginate microcapsules has been used in agriculture for the controlled release of nutrients [17] and the release oil to heal the cracking of asphalt [51]. For the purpose of this research, when subjected to a wetting–drying cycle, calcium alginate swells and shrinks. These volumetric changes are related to changes of water content and pH [4]. Here, as shown in Fig. 1, we hypothesize the hydrophobic cargo is released during shrinkage driven by drying, inducing or enhancing hydrophobicity in the soil, and eventually leading to the depletion of the microcapsules' hydrophobic cargo during successive wetting and drying cycles. To test the hypothesis, the microcapsules behavior was tested under a drying path and wetting–drying cycles. The drying path provides details about the microcapsules' behavior during drying (shrinkage and cargo release). The wetting–drying cycles simulate the process of soil

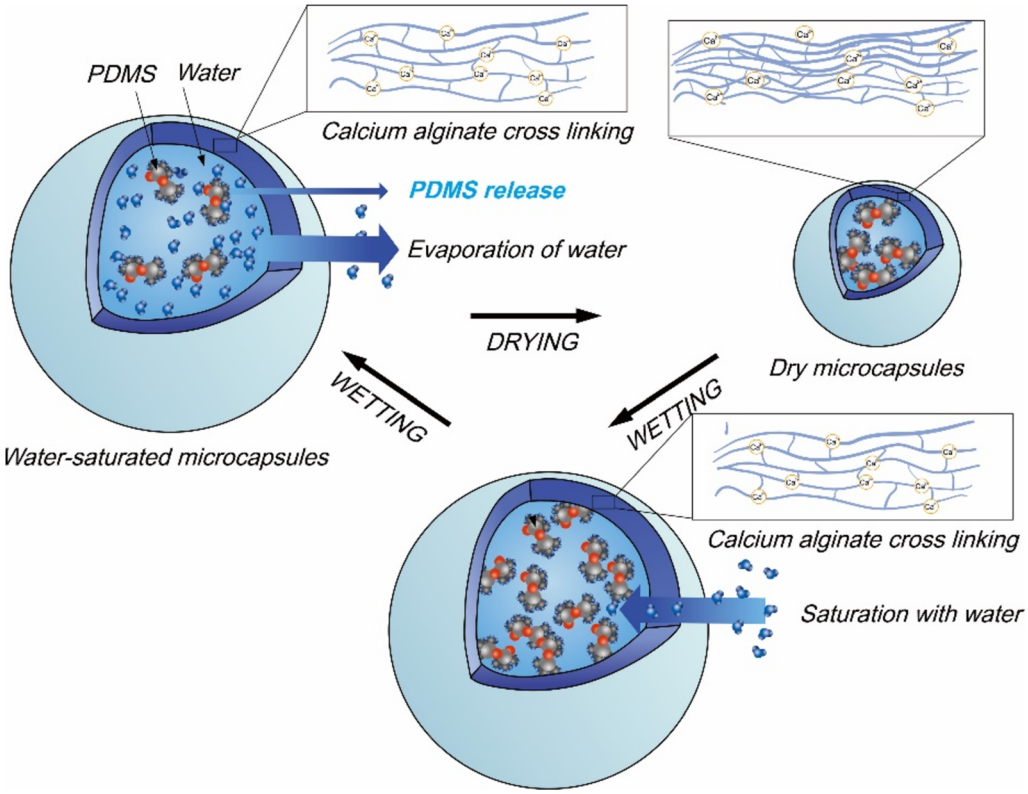

Fig. 1 Conceptual diagram for imparting hydrophobicity in sands with microcapsules and release mechanism of PDMS cargo from calcium alginate microcapsules following drying and wetting paths

hydrophobicity degradation and subsequent recovery. In practical terms, the hydrophobized soils are expected to remain dry during their working life. Saturation occurs as hydrophobicity decreases and water breakthroughs into the pores. Therefore, in this study, after drying, the microcapsules were separated and saturated or flooded by water, simulating practical scenarios where microcapsules experience wetting after soil hydrophobicity degradation.

The aim of this study is to test the potential of microencapsulation to impart hydrophobicity in soils in a response to a stimulus or trigger. Specific objectives are (1) to synthesize calcium alginate microcapsules with PDMS cargo by the ionic gelation method, (2) to investigate the release behavior of PDMS under a single stimulus (a drying path) or multiple consecutive stimuli (wetting–drying cycles), and (3) to verify the effectiveness of microcapsules in enhancing soil hydrophobicity. The results will inform the extent of hydrophobic recovery, relative timescales and controlling mechanisms. These datasets will then provide the foundations to design granular materials-microcapsules systems to extend the longevity of hydrophobized soils or to design smart infrastructure *i.e.,* that switches to hydrophobic in response to drying and wetting episodes.

2 Materials and methods

2.1 Fine sands as host material

Fine quartz Fujian sand with a particle size ranging from 150 to 300 μm was used. PDMS is effective in inducing high and persistent hydrophobicity in quartz sands [35] as it provides repeatable and reproducible results. The finer particle size was selected to allow the measurement of higher contact angles [45]. For application in natural soils with variable grain size and composition, both PDMS and fatty acids (e.g.,, tung oil) are potential candidates [27, 36].

2.2 Synthesis of microcapsules

Calcium alginate microcapsules will be produced by ionic gelation which has proven effective to synthesize such microcapsules and release organic acids in soils [26]. As a natural polysaccharide, alginate has the advantage of being biodegradable, biocompatible and non-toxic [56]. Polydimethylsiloxane (PDMS), a silicone, can induce high and stable hydrophobicity in sands and will be used as the hydrophobic cargo [34]. PDMS can degrade in soils via a combination of hydrolysis, oxidation, and microbial processes [29] and is therefore safe to use in soils. The ionic

gelation method is a commonly used encapsulation method in agriculture for the controlled release of nutrients [50]. The method is based on the cross-linking of sodium alginate with calcium ion cations [14, 38]. Sodium alginate is composed of two glycan monomers β-d-mannuronic acid and a α-l-guluronic acid [2]. The divalent cations (Ca^{2+}) interacted ionically with blocks of guluronic acid residues of sodium alginate, resulting in the formation of a three-dimensional network (cross-linking process) of calcium alginate which performs as the shell of microcapsules.

Sodium alginate ($NaC_6H_7O_6$) and calcium chloride ($CaCl_2$) (Sigma-Aldrich) were used to form the shell. PDMS is in a liquid form and its density is 965 kg/m^3 (Acros Organics). The encapsulation method workflow is depicted in Fig. 2. The microcapsules were synthesized in a series of steps: *(1) Preparation of sodium alginate solution:* Sodium alginate was firstly dissolved in deionized water with an overhead steerer (IKA RW20 digital, Germany) at 200 rotations/min. The proportion, 1.5/100, which is the mass of sodium alginate to the mass of distilled water and PDMS, was used in the experiments. *(2) Preparation of PDMS sodium alginate emulsion:* PDMS was added into the sodium alginate solution and emulsified with a high-speed homogenizer (Benchmark, D1000) at 1200 rotations/min until a stable oil–water emulsion was formed. The mass of PDMS used per 100 g distilled water in the encapsulation process is defined as 'PDMS loading'. The PDMS loading is limited by the syringe needles used in the encapsulation process. High PDMS loading leads to blocking of the syringe needles compromising the encapsulation process. Alternatively, dripping the $CaCl_2$ solution into sodium alginate emulsion is not advisable due to challenges associated with maintaining precise control over the size and shape of the resulting capsules. In this study, microcapsules with three PDMS loadings (5 g, 10 g, 20 g to 100 g deionized water) were produced to identify the optimum PDMS loading to assess the healing effect of microcapsules. *(3) Formation of microcapsules:* The emulsion droplets were then dripped into a calcium chloride solution (1.0 M) through a PTFE tube by means of a syringe pump (KD Scientific). The dripping speed was set as 2 ml/min, which allowed stable PDMS and sodium alginate droplets. The calcium chloride solution was prepared by dissolving 110.98 g calcium chloride powder into 1000 g distilled water. The sodium silicate cross-linked and encapsulated the PDMS by dripping the PDMS and sodium alginate emulsion into the $CaCl_2$ solution. The size of the syringe needles influences the size of microcapsules. Thus, three different syringes needles with an inner diameter of 0.16 mm, 0.25 mm and 0.3 mm were used to produce microcapsules with different diameters. *(4) Filtering:* After the microcapsules were produced, they were immersed in the calcium chloride solution bath for 24 h, rinsed with distilled water, and filtered with a vacuum pump (LongerPump WT3000-1JB, China). The microcapsules were then air-dried at the ambient temperature (∼ 25 °C) for 12 h, which allows the evaporation of water on the surface of the microcapsules.

2.3 Characterization of microcapsules

Scanning electron microscopy (SEM) (Zeiss LEO, 1530 FEG) was used to image the dried microcapsules in order to provide qualitative information on their morphology. The microcapsules were sprayed with gold powder to conduct electricity and scanned at a voltage of 5 kV. The size of the microcapsule with air-drying was recorded. The size and shape of microcapsules were characterized by a dynamic image analyser (QicPic^{TM}, Sympatec GmbH). 5 g of microcapsules samples were analyzed to obtain the 50% median values (D_{50}) of microcapsules size and shape. The thermal stability of the microcapsules was measured with a thermogravimetric analyzer. Approximately 5 mg of microcapsules were heated in a PerkinElmer TGA 4000

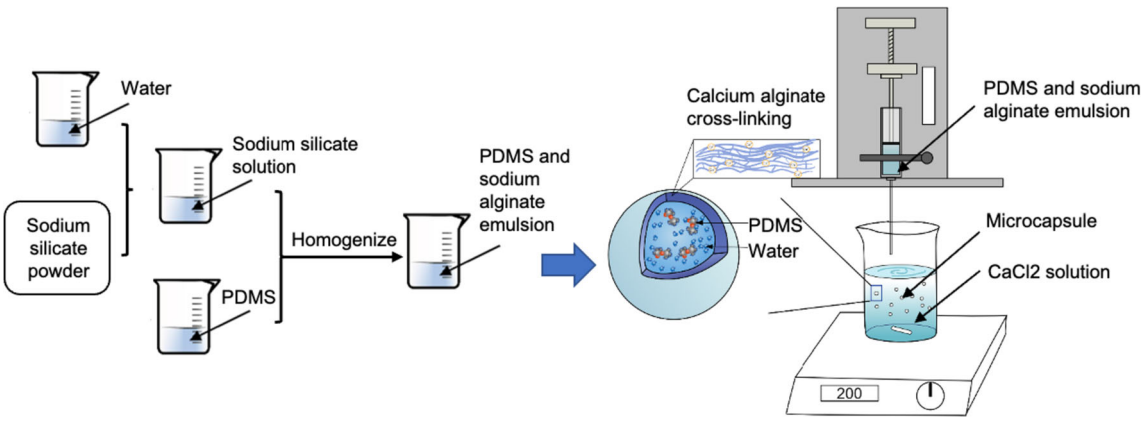

Fig. 2 Encapsulation process with the ionic gelation method

system, from 25 to 950 °C with a heating rate of 20 °C/min in N_2 flow (20 ml/min). A PerkinElmer Frontier IR single-range spectrometer was also used to measure the molecular structure of the core material (PDMS) and microcapsules' shell.

2.4 Hydrophobicity measurement

Soil hydrophobicity can be quantified by the contact angle (CA) and water drop penetration time (WDPT) [36]. The CA reflects the severity or degree of soil hydrophobicity.Through Young–Laplace equation, a contact angle 90° is used as a threshold, above which the soil can be classified as hydrophobic [25]. WDPT measures the infiltration rate of a water drop into the soil and thus indicates the persistency of soil hydrophobicity [33].

The sessile drop method [3] was used to measure the CA of the sand specimens. A 10 μL drop of water was dispensed on the sand surface and the CA was recorded with a drop shape analyser (DSA100, KRÜSS GmbH). WDPT was measured by dispensing water drops with a volume of 50 μL with a pipette onto the surface of the sand [34] and timing their infiltration.

2.5 PDMS release behavior under a drying path

The release behavior of PDMS with time and the induced hydrophobicity in the sand were investigated. The procedures were as follows: (1) Microcapsules were mixed with Fujian sand and left in ambient laboratory conditions (∼ 25 °C, ∼ 60% relative humidity) until further use. The microcapsules were not completely dried and the initial water content ranged from approximately 65%, 70%, to 80%, depending on the PDMS loading (20, 10, and 5, respectively). The sand used in the experiments was initially dried, possessing a water content of 0%. The ratio of mass of microcapsules to the mass of sand is defined as 'capsule density' with three microcapsules density (4%, 8% and 12%) investigated. Preliminary testing revealed that 8% microcapsule density in the soil can induce high and stable hydrophobicity. For comparison purposes, density values above and below were selected (4% and 12%) to investigate the effect of microcapsule density on soil hydrophobicity enhancement and recovery. (2) The sand and microcapsules were separated with sieves in the 1st day, 3rd day, 6th day, 12th day and 24th day, where the moisture content and PDMS content of the separated sand sample as well as the sand hydrophobicity through the CA and WDPT were measured. The drying times were selected based on the shrinkage of microcapsules during drying. As shrinkage stabilized on the 12th day, the maximum testing duration was set as the 24th day in order to capture any residual changes of the microcapsules volume. The influence of PDMS loading and the capsule density were investigated to indicate the optimal conditions to induce hydrophobicity in soils. Sand moisture content was measured by drying samples at a temperature of 105 °C. Mass measurements of sand moisture and PDMS were conducted in an analytical balance with readability 0.01 mg (Sartorius, Secura 225D-1S). The PDMS content was measured by thermogravimetric analysis by heating the sand to 850 °C, as PDMS has been reported to have an 85% mass loss in these tests [37, 46]. The CA and WDPT of sand were also measured with the methods mentioned above. For each experimental group, three replications were conducted to obtain the standard deviation.

2.6 PDMS release behavior under wetting–drying cycles

The release behavior of PDMS from microcapsules into the sand under wetting–drying cycles and the respective hydrophobic recovery were investigated. Testing was conducted with the microcapsules prepared at three different PDMS loadings (5 PDMS, 10 PDMS, and 20 PDMS) added to Fujian sand (150 g) at three different microcapsules density (4%, 8% and 12%). All tests initiated with the sand-microcapsule system in a water saturated condition. The water saturated environment was kept for 2 days followed by air-drying (∼ 25 °C, ∼ 60% relative humidity) for 5 days; after this time there is no further release of PDMS. Note that 5-days does not imply the microcapsules were in a dried state (water content = 0%), only that PDMS did not further release beyond this time frame. The microcapsules and sand were separated after each wetting–drying cycle. The separated microcapsules were mixed with another 150 g sand and subjected to another wetting–drying cycle while the separated sand samples were used for the measurements of the moisture content, PDMS content, CA and WDPT. Samples were subjected to a total of ten wetting–drying cycles. For each experimental group, three replicates were conducted to obtain the standard deviation.

3 Results and discussion

3.1 Characterization of microcapsules

3.1.1 Size and shape

Figure 3 shows the SEM image of representative dried microcapsules. Wrinkles can be observed in the surface suggesting shrinkage after air-drying. The microcapsule's median diameter change (D_{50}) with air-drying time is shown in Fig. 4. Once the microcapsules were produced,

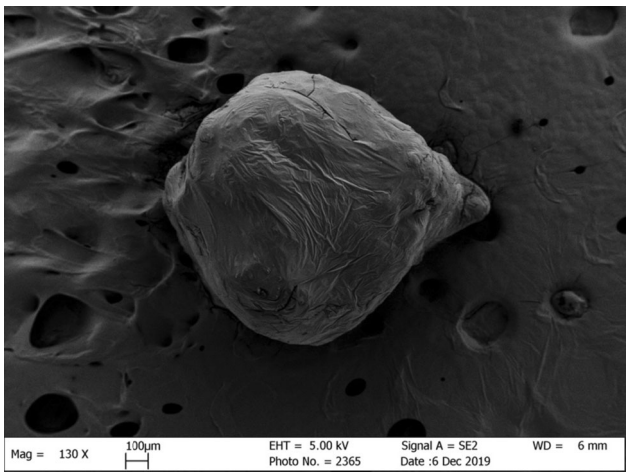

Fig. 3 Microphotograph of single dried microcapsules (20 PDMS loading) by scanning electron microscopy

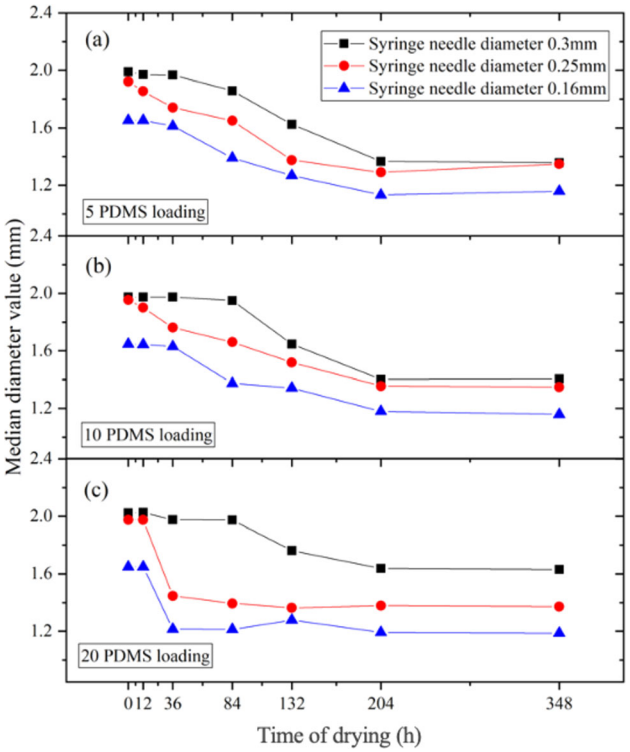

Fig. 4 Diameter change of microcapsules with time: **a** 5 PDMS loading; **b** 10 PDMS loading; **c** 20 PDMS loading

the initial size of microcapsules with different PDMS loading (5, 10 and 20 PDMS loading) and different syringe needle diameter (0.16 mm, 0.25 mm, and 0.3 mm) is in the range of 1.60 mm to 2.10 mm (Fig. 4a–c). For instance, microcapsules produced by the 0.3 mm syringe needle had the largest initial size: from 1.99 to 2.02 mm. The initial size of microcapsules produced by 0.16 mm syringe needle was smaller at ~ 1.65 mm. With air-drying, the size of microcapsules decreased to a range between 1.10 and 1.70 mm. The syringe needle diameter is the most important factor contributing to the final size of microcapsules after air-drying with the PDMS loading assuming a minor role. For the dried microcapsules, with increasing syringe needle diameter, the size of microcapsules also increased. For example, the median diameter of 5 PDMS loading microcapsules (Fig. 4a) produced by 0.16 mm syringe diameter was 1.16 m, while when the syringe diameter increased to 0.30 mm, the average diameter of produced microcapsules increased to 1.36 mm. Also, a greater PDMS loading resulted in a larger microcapsules size after air-drying. For example, for a syringe needle diameter = 0.3 mm, the average diameter of 5 and 20 PDMS loading microcapsules was 1.36 and 1.67 mm, respectively (Fig. 4a, c).

Two factors control the size of microcapsules after air-drying: the initial dimension of droplets and shrinkage during the air-drying process. The initial dimension mainly depends on the size of the emulsion droplets (stage 3 of the synthesis procedure) before adding to the calcium chloride solution. As a result, the falling height of the droplets, the pumping speed as well as the diameter of the syringe needle affects the droplet size and finally influences the initial diameter of the microcapsules [13]. The shrinkage of microcapsules is driven by water evaporation and mostly controlled by the PDMS loading, related to the ratio of PDMS to water in the microcapsules. For a lower PDMS loading, the proportion of water within the microcapsules is greater resulting in a large mass loss during drying and consequently in a greater microcapsule's shrinkage.

The retention of microcapsules in soils under the influence of seepage water is proven to be related to the particle size distribution of the microcapsules and the host soils. Based on the washout test of microcapsules, a constriction size-based criterion was proposed by Chen et al., whereby for a size of microcapsules ranging from 1.60 to 2.10 mm, and the size of the host soil particles ranging from 0.15 to 0.3 mm, the flushing away percentage of microcapsules in soils under seepage water was less than 0.07% (99.93% of retention rate) [15].

3.1.2 Thermal stability

The thermal stability of microcapsules is an important property to (1) evaluate the microcapsules behavior under seasonal soil temperatures (10–40 °C, Hong Kong [16]), (2) to assess the decomposition of the shell material and cargo and, (3) to evaluate the proportion of cargo encapsulated. The thermal gravimetric analysis for mass loss of blank microcapsules and microcapsules with encapsulated PDMS is shown in Fig. 5a. For blank microcapsules, the thermal degradation processes were related to (1) dehydration (25–100 °C), (2) calcium alginate decomposition

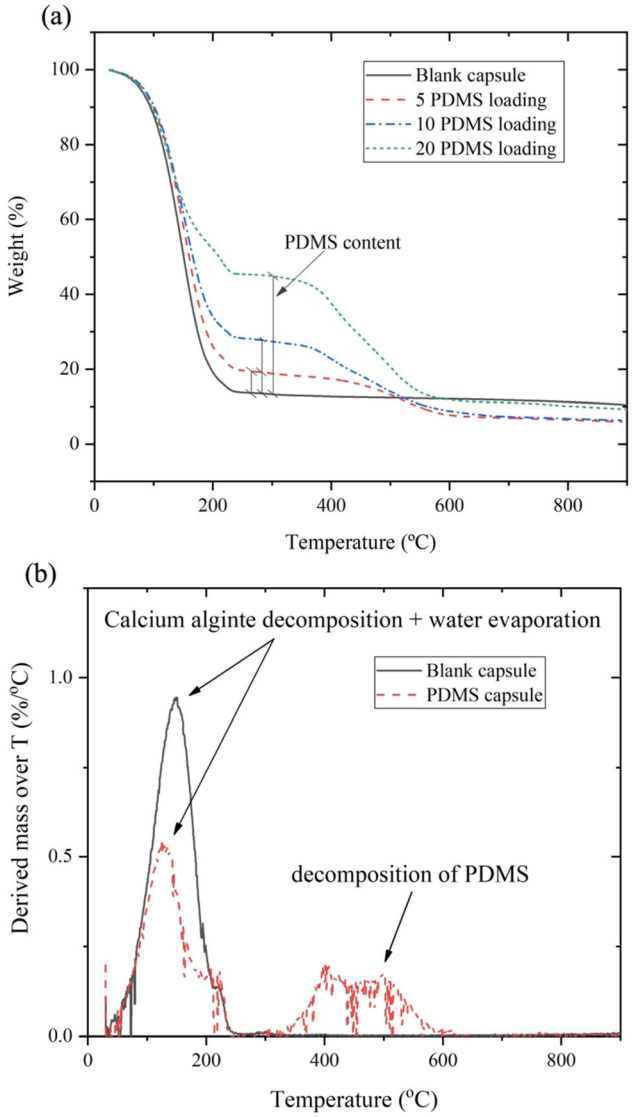

Fig. 5 Thermogravimetry analysis of microcapsules: **a** thermogravimetry analysis of microcapsules at different PDMS loadings; **b** derivative thermogravimetric (DTG) curves of blank and PDMS microcapsules

(170–350 °C), and (3) carbon volatilization (350–800 °C) [1]. For microcapsules at variable PDMS loading, there were four steps of mass loss: (1) water evaporation (25–100 °C), (2) calcium alginate decomposition (170–350 °C), (3) decomposition of PDMS (400–600 °C), and (4) carbon volatilization (350–800 °C). Using the blank microcapsules as a baseline, the height of the flat range of the curves indicates the proportion of PDMS encapsulated in the microcapsules.

The endothermic curves of blank microcapsules and microcapsules with encapsulated PDMS is shown in Fig. 5b. Two endothermic temperature ranges can be detected (around 240 °C and 400 °C to 600 °C). The initial endothermic range is shared with the blank microcapsules, which corresponds to the evaporation of water and decomposition of calcium alginate. The second endothermic region corresponds to the decomposition of PDMS in the range 400 °C to 600 °C.

FTIR was also used to assess the presence of characteristic groups in the microcapsules [12]. Figure 6 shows the FTIR results of PDMS (Fig. 6a) and microcapsules with PDMS core (Fig. 6b). PDMS exhibits peaks at 789–796 cm^{-1} (–CH_3 rocking and Si–C stretching in Si–CH_3), 1020–1074 cm^{-1} (Si–O–Si stretching), 1260–1259 cm^{-1} (CH_3 deformation in Si-CH_3), and 2950–2960 cm^{-1} (asymmetric CH_3 stretching in Si–CH_3) [28] indicating that PDMS had been encapsulated.

3.2 PDMS release behavior under air-drying and sand hydrophobic enhancement

3.2.1 PDMS release

Figure 7a shows that the PDMS content released into the sand increases with time. As stated, microcapsules with three PDMS loadings and three capsule densities were used. The PDMS content in sand is assumed to be equal to the amount of PDMS being released from the microcapsules. For example, as shown in Fig. 7a, for sands mixed with 10 PDMS loading and 12% capsule density, the PDMS content increased to 0.31% after 24 h and eventually reached 0.63% on the 24th day. As shown in Fig. 7a, most PDMS release occurs in the initial days. In average, the releasing amount accounted for 59.9% of the total release during the testing period. In other words, the

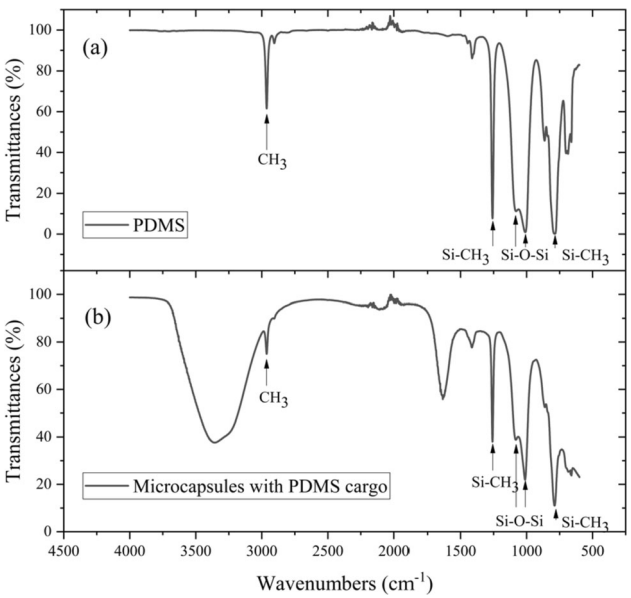

Fig. 6 Fourier-transform infrared spectroscopy of PDMS and microcapsules with PDMS cargo

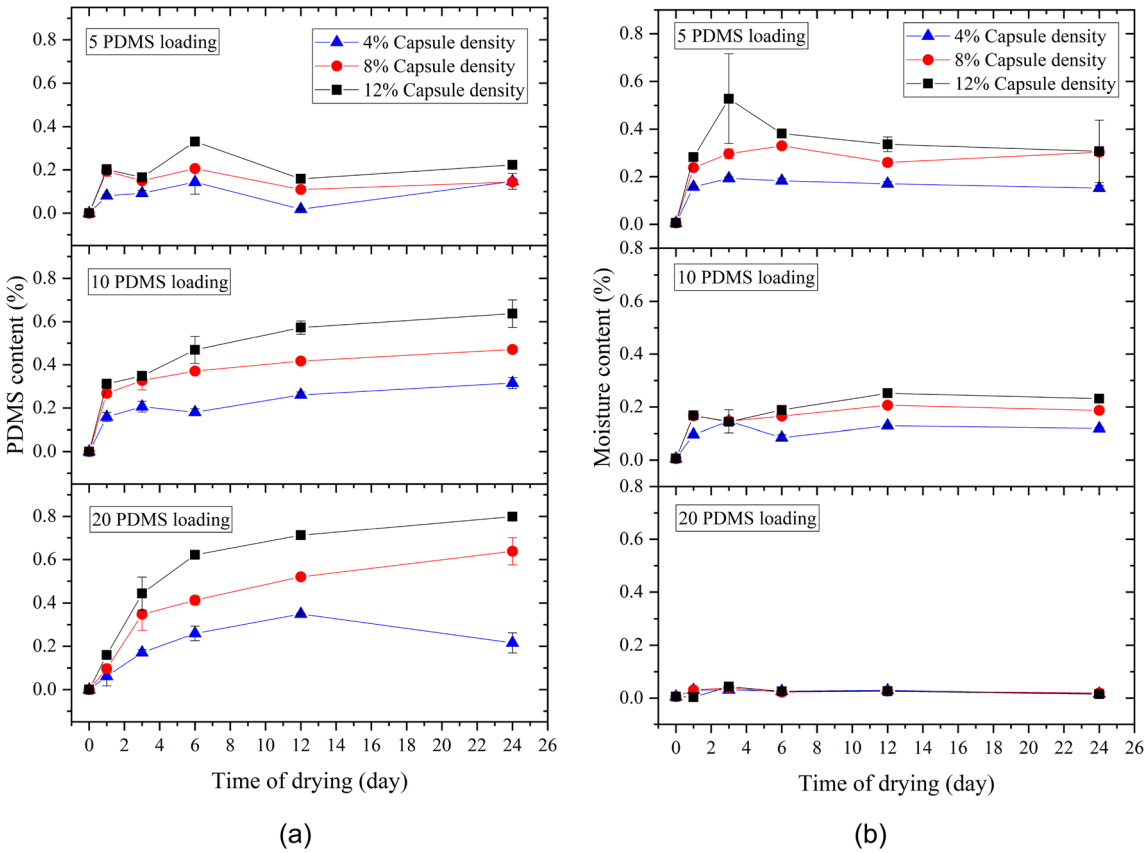

Fig. 7 PDMS release and sand moisture content with time for samples prepared at 5, 10, 20 PDMS loading and 4%, 8%, 12% capsules density; **a** PDMS release; **b** moisture content in sand

releasing rate was higher in the initial days, decreasing Afterward. With continuous drying of microcapsules, the shell densifies, hindering the cargo movement from the core of the capsule to outside.

PDMS loading and capsule density influenced the PDMS content in the sand. As shown in Fig. 8a, for sand mixed with microcapsules with 12% capsule density and increasing PDMS loading (5, 10 and 20 PDMS loading), the PDMS contents also increased, from 0.22, 0.64% to 0.80%, respectively. As shown in Fig. 8b, as the capsule density increased from 4 to 8% and 12%, PDMS content on the 24th day increased from 0.32% to 0.47% and 0.64%, respectively (10 PDMS loading). The experimental group with the highest PDMS loading and capsule density had the highest PDMS content in the sand. For example, 20 PDMS loading and 12% capsule density reached 0.80% in the 24th day, which was higher than the other groups.

3.2.2 Sand moisture content

The moisture content in sand was measured as it is known to influence soil wettability, by switching a soil to hydrophilic above a critical moisture content [36]. Figure 7b shows the change of moisture content in sands with time. The moisture content increased as the microcapsules dried, due to the release of water from the microcapsules. As shown in Fig. 8c, d, sands mixed with a lower PDMS loading and a higher capsule density had a higher moisture content because for a decrease of PDMS loading, the proportion of water in the microcapsules increased. Sand samples mixed with microcapsules at 5 PDMS loading and 12% capsule density had the highest sand moisture content, which was 0.31% on the 24th day.

3.2.3 Sand hydrophobic enhancement

The CA was measured in the sand after the release of PDMS (Fig. 9a). The CA of clean sand was 29.7 ± 0.77° and increased with time with a higher rate of increase initially. For example, as shown in Fig. 9a, for 5 PDMS loading and 4% capsule density, the CA increased significantly to 87.3° on the 1st day and eventually reached 89.8° on the 24th day. Two reasons may explain the significant increase initially. On the one hand, a small amount of PDMS can induce a large CA increase for an originally hydrophilic sand. On the other hand, the release amount of PDMS from the microcapsules was also greater at the beginning.

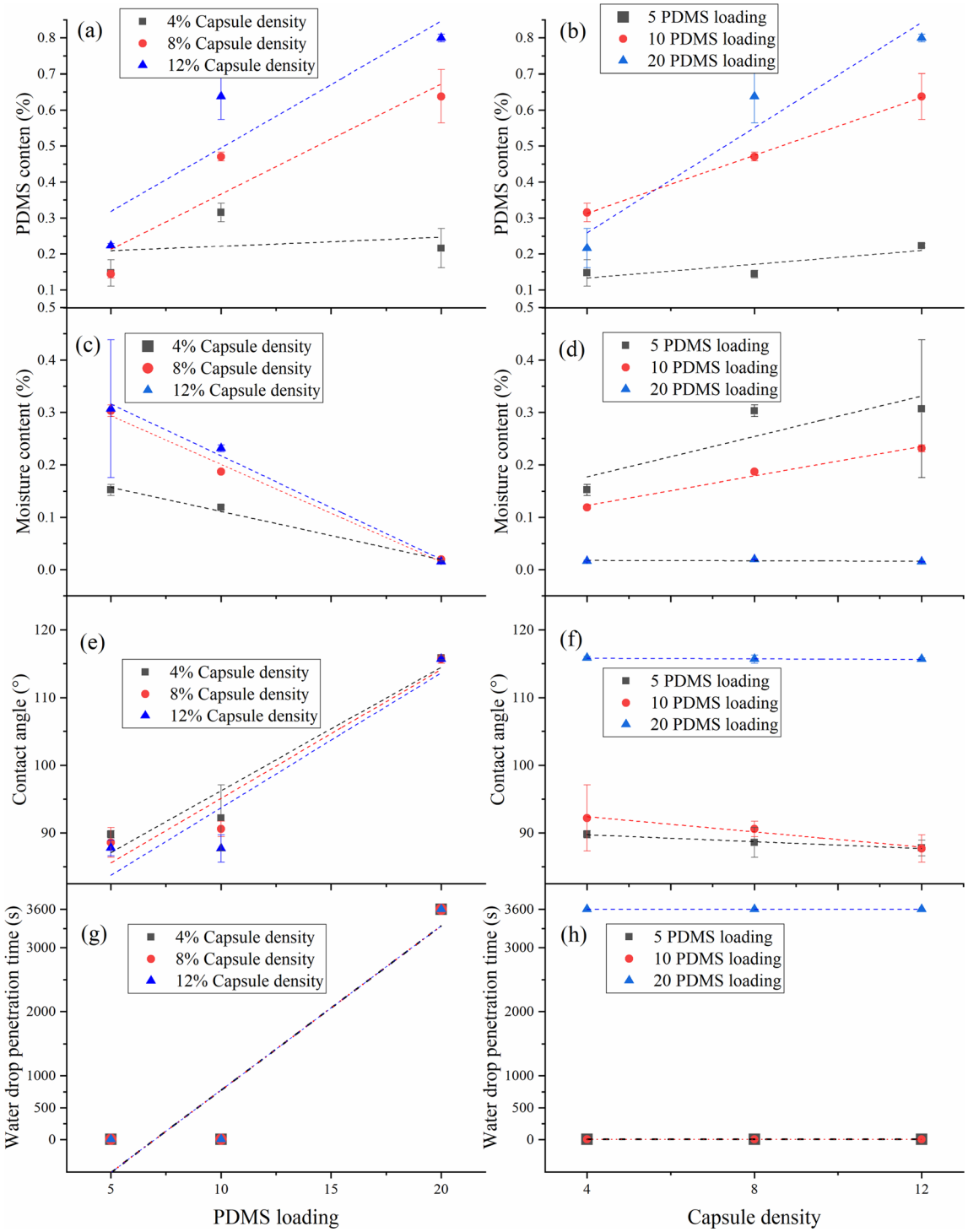

Fig. 8 Effect of PDMS loading on **a** PDMS release; **c** moisture content in sand; **e** contact angle; **g** water drop penetration time during drying. Influence of capsules density on **b** PDMS release; **d** moisture content in sand; **f** contact angle; **h** water drop penetration time during drying

The CA increased with PDMS loading (Fig. 8e). For the experimental group with 4% capsule density, the CA on the 24th day was 89.8°, 92.2° and 115.8° for 5, 10 and 20 PDMS loading, respectively. However, the CA does not increase with the increase of capsule density, on the contrary, a slight decrease was measured. As shown in Fig. 8f, for the experimental group with 5 PDMS loading, the CA on the 24th day was 89.8°, 88.6° and 87.7° for a capsule density 4%, 8% and 12%, respectively. The CA was 92.2°, 90.6° and 87.7° for the 10 PDMS loading

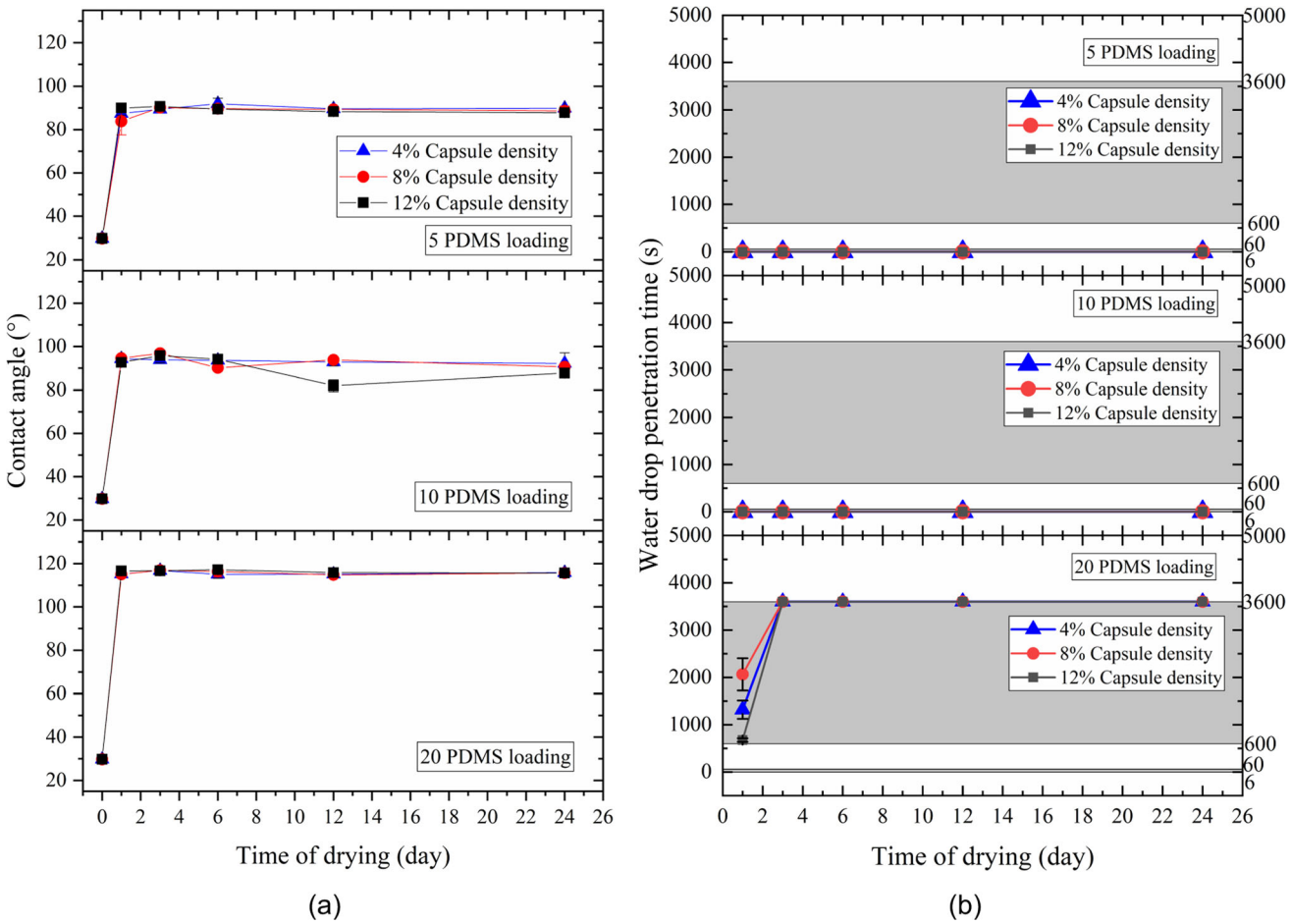

Fig. 9 Sand hydrophobicity with time for samples prepared at 5, 10, 20 PDMS loading and 4%, 8%, 12% capsules density: **a** contact angle; **b** water drop penetration time

experimental group and 115.8°, 115.6°, 115.6° for 20 PDMS loading, at the same capsules' density. Hydrophobicity (via the CA) not only depends on its intrinsic value (107° for PDMS) but is also affected by other factors such as particle size and sand moisture content. The adsorption of water to hydrophobic sand surfaces, which is related to the increase of moisture content, can increase the net surface free energy of the sand and weaken hydrophobicity [32]. As shown in Fig. 8b, d, f, although the PDMS content and moisture content in sand increased with increasing of capsule density, hydrophobicity decreased. For example, for experimental groups with higher capsule density (12% capsule density, 10 PDMS loading), both PDMS content and moisture content were higher, at 0.64% and 0.23%, respectively, but hydrophobicity decreased.

Figure 9b shows the WDPT results of sand after removal of the microcapsules. WDPT was less than 5 s for samples with 5 PDMS loading and 10 PDMS loading, indicating a negligible persistence of hydrophobicity. WDPT at 20 PDMS loading increased to 1320 s, 2064 s and 676 s at 4%, 8%, 12% capsule density, respectively, on the 1st day. From the 3rd day, the WDPT at 20 PDMS loading exceeded 3600 s, indicating an extreme and persistent hydrophobic state.

Differences between soil CA and WDPT may be attributed to the methods followed and percentage of PDMS cover of sand grains. CA measurements are typically conducted as soon as a neat image of the three-point interface (solid–air–water) is obtained. This is done in order to minimize the droplet bouncing, spreading and infiltration after placing on the sample. As a result, CA measurements will tend to be higher. On the opposite, the low WDPT for 5 and 10 PDMS loading could be interpreted as a partial or patchy cover of grains with PDMS, resulting in a greater spreading of the water meniscus on the surface of the grains, thus resulting in lower persistency.

3.3 PDMS release behavior under wetting–drying cycles and sand hydrophobic enhancement

3.3.1 PDMS release

Figure 10a shows the content of PDMS in sand mixed with microcapsules with 5, 10 and 20 PDMS loading after each wetting–drying cycle. Since the PDMS content in sand represents the PDMS release amount from microcapsules at each wetting–drying cycle, the release of core material decreased with the increase of wetting–drying cycles. As shown in Fig. 10a, for microcapsules with 5 PDMS loading, after the initial wetting–drying cycles, PDMS content in sand was 0.06%, 0.15% and 0.20% for 4%, 8%, 12% capsule density, respectively. After ten wetting–drying cycles, the PDMS content reduced to less than 0.02%. PDMS content in sands mixed with 20PDMS loading is the highest, from 0.18%, 0.44% and 0.40% in the first wetting–drying cycle, gradually decreasing to 0.04%, 0.09% and 0.15% on the 10th wetting–drying cycle (for 4%, 8%, 12% capsule density, respectively).

The PDMS content in sand increased with capsule density. For example, in Fig. 10a, after the initial wetting–drying cycles, as the capsule density increased from 4 to 12%, the PDMS content increased from 0.16 to 0.35% (10 PDMS loading). The average PDMS release for all wetting–drying cycles for 4% capsule density and 8% capsule density were 2.55 × , 2.17 × , and 2.62 × (for 5, 10, 20 PDMS loading, respectively), while for 8% capsule density and 12% capsule density, the relationships were 1.99 × , 1.51 × , and 1.41 × (5, 10, 20 PDMS loading). In relative terms, considering the experimental errors, the PDMS content in the sand at 8% capsule density was approximately 2 × higher than 4% capsule density, and for 12% capsule density was approximately 1.5 × higher than 8% capsule density, indicating that the releasing amount of PDMS by a single microcapsule under wetting–drying cycles was similar, with the number of microcapsules controlling the total PDMS content in the sand.

From Fig. 10a, for the same capsule density, a higher PDMS loading also achieved a higher PDMS content with wetting–drying cycles. For example, for 8% capsule density, as the PDMS loading of microcapsules increased from

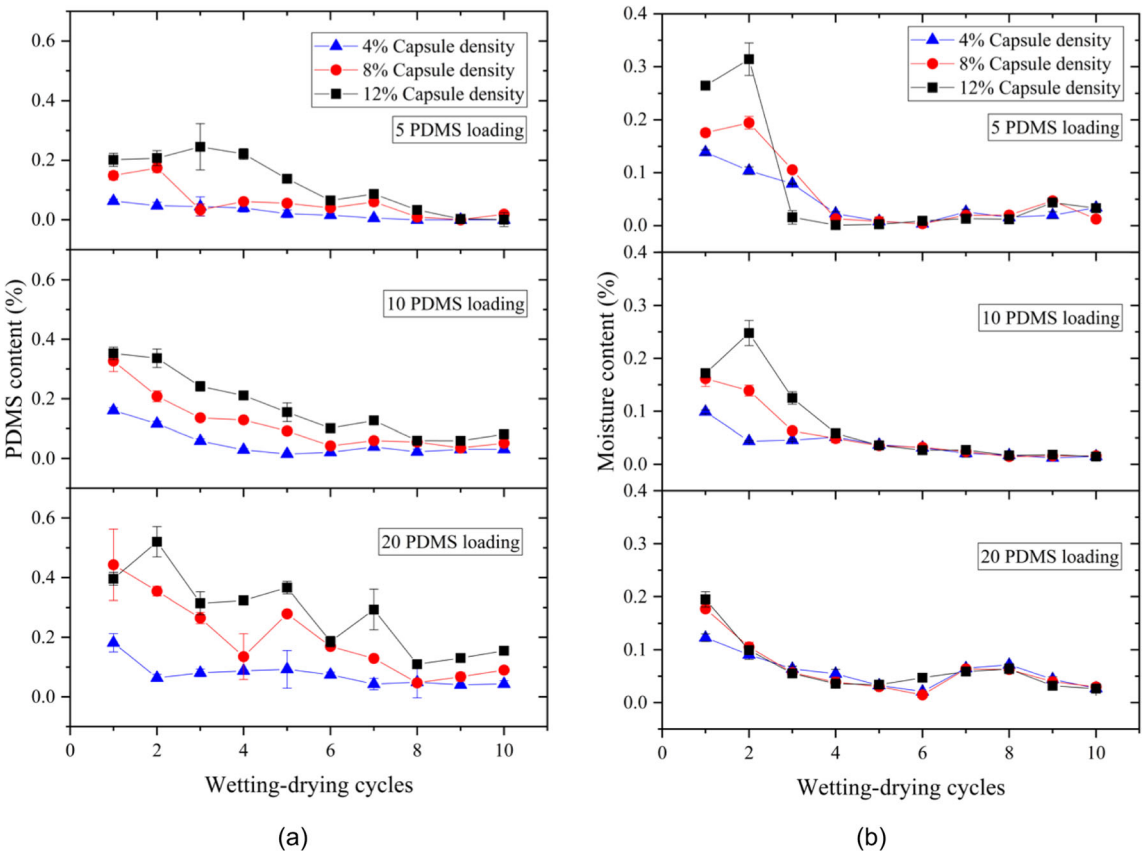

Fig. 10 PDMS release and sand moisture content with wetting–drying cycles under 7 days of typical wetting–drying duration (2 days of wetting and 5 days of drying) for samples prepared at 5, 10, 20 PDMS loading and 4%, 8%, 12% capsules density; **a** PDMS release; **b** moisture content in sand

5 to 10 and 20, the released PDMS amount after the 3rd wetting–drying cycle was 0.03%, 0.14% and 0.26%, respectively. This demonstrated that the release amount of core material from a single microcapsule is higher as the PDMS loading increases. In other words, the PDMS loading can change the release ability of single microcapsules in the wetting–drying process. This can be explained by the microcapsule's synthesis, where the increase of PDMS loading leads to a decrease in the proportion of sodium alginate resulting in a weaker crosslinking structure which might amplify the ability of PDMS to percolate from the inside to the outside of the microcapsules.

3.3.2 Sand moisture content

Figure 10b shows the sand moisture content after wetting–drying cycles. With the increase of wetting–drying cycles, the moisture content after air-drying decreased. The moisture content in the first three wetting–drying cycles was significantly higher than the remaining cycles. For example, for 5 PDMS loading (Fig. 11a), the sand moisture content in the first wetting–drying cycle was 0.14%, 0.18%, 0.26% (for 4%, 8%, 12% microcapsules density, respectively), decreasing to < 0.03% in the 4th wetting–drying cycle. Experimental groups with 10 PDMS loading and 20 PDMS loading showed similar trends.

3.3.3 Sand hydrophobic enhancement

Figure 11a shows the CA's after each wetting–drying cycle. With the increase of wetting–drying cycles, the CA's increased at first followed by a decreased. For example, for 5 PDMS loading with 4% capsule density, the CA increased to 93.2° after the second wetting–drying, decreasing to 74.2° after the 10th wetting–drying cycle. As PDMS loading increased, sand hydrophobicity increased with wetting–drying cycles. As the capsule's density increased, the CA was lower in the first three wetting–drying cycles and higher after the 4th wetting–drying cycle.

Figure 11b shows the WDPT after wetting–drying cycles. Similarly, the WDPT increased with wetting–drying cycles at first and then decreased. For the experimental

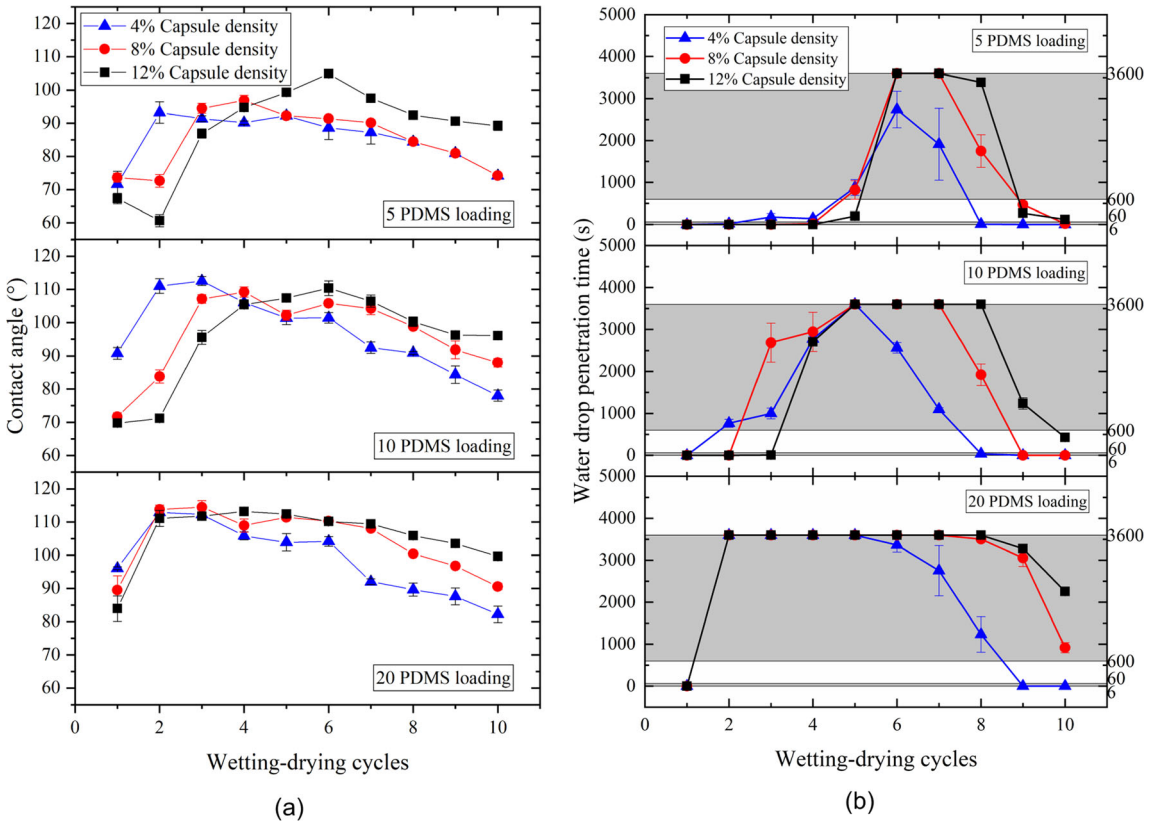

Fig. 11 Sand hydrophobicity with wetting–drying cycles under 7 days of typical wetting–drying duration (2 days of wetting and 5 days of drying) for samples prepared at 5, 10, 20 PDMS loading and 4%, 8%, 12% capsules density; **a** contact angle; **b** water drop penetration time

group with 5 PDMS loading, WDPT increased from less than 5 s (after the first wetting–drying cycles) to 880 s, 820 s, 199 s (for 4%, 8% and 12% capsule density, respectively) after the 5th wetting–drying cycle, which shows the sand switching to hydrophobic. Sand hydrophobicity becomes persistent (WDPT > 2000 s) in the 6th wetting–drying cycle. As PDMS loading increased, hydrophobicity becomes more persistent in the initial wetting–drying cycles. For instance, for 10 PDMS loading, WDPT is greater than 3600 s from the 5th wetting–drying cycle and from the 2nd wetting–drying cycle for 20 PDMS loading. Afterward, WDPT decreases with an increase of wetting–drying cycles. For 5 PDMS loading, WDPT reduced to 500 s on the 8th wetting–drying cycle (4% capsule density), while for the experimental group of 8% and 12% capsule density, it decreased to 500 s after the 9th wetting–drying cycle. A similar decrease took place for 10 and 20 PDMS loading.

As revealed by the results, both CA and WDPT were affected by the PDMS release and sand moisture content. Although more PDMS was released in the initial wetting–drying cycles, the moisture content was also higher, explaining why experimental groups with higher microcapsules density had a lower CA and WDPT. For experimental groups with higher PDMS loading, the PDMS release amount is higher and the moisture content in sand is lower, resulting in a higher CA and WDPT.

3.4 Release mechanism and implications for use in ground infrastructure

A release mechanism of hydrophobic cargo from microcapsules during air-drying and wetting–drying cycles is proposed in Fig. 1. The mechanisms of cargo release from microcapsules include diffusion, dissolution, osmosis and erosion [47]. In this study, the release mechanism is assumed to be driven by shrinkage during air-drying with the cargo percolating through the shell pores. With continuous drying, the microcapsules shrunk to ~ 70% of their original diameter. The microcapsules shell structure densifies which further hinders the release of cargo from the microcapsules. In the subsequent wetting stage, water is re-absorbed into the system and the microcapsules swell to ~ 75% of the original diameter according to a previous study [42]. The swollen microcapsules can further release cargo as the environment switches from wet to dry until all PDMS is released in the subsequent wetting–drying cycles. Deformation-driven mechanisms have also been proposed for asphalt [5, 43].

This study has demonstrated that controllable hydrophobization of sands by microencapsulation is feasible in the laboratory. Microcapsules mixed with sand, release hydrophobic cargo with air-drying, imparting hydrophobicity in originally hydrophilic soils. In infrastructure, hydrophilic or hydrophobic sands can be mixed with microcapsules loaded with hydrophobic cargoes and placed at soil-structure or soil-atmosphere interfaces to respond as barriers to wetting. Hydrophobic barriers provide a dry environment that can preserve microcapsules with hydrophobic cargoes. As soon as pore water reaches the microcapsules, they will saturate and release the hydrophobic cargo in the subsequent air-drying episode. Consecutive air-drying events will then enable the re-release of the hydrophobic cargo leading to a gradual built-up of hydrophobicity and switching the soil from hydrophilic to hydrophobic.

From this study, microcapsules can endure 10 wetting–drying cycles and still release hydrophobic cargo and induce hydrophobicity on the last cycle. Notwithstanding the exploratory and experimental nature of this study, similar functional times to recover soil hydrophobicity could be achievable in infrastructure. As for the optimal conditions to deploy microcapsules in the field, since a higher loading increases hydrophobicity while a lower capsules density limits the increase in soil moisture, based on the results, 20 PDMS loading, and 8% capsule density represents the best combination to deploy microcapsules in infrastructure.

3.5 Limitations and future work

As for differences between the laboratory and field application, in the field, hydrophobic recovery would represent a cumulative increase by successive additions of hydrophobic cargo in the same soil, rather than a continuous release in a fresh hydrophilic soil, as tested here. Therefore, further work is needed to ascertain possible differences with this study. In addition, for soil hydrophobicity induced by polymers (e.g., organo-silanes, fatty acids), there is a critical value after which the polymer content does not further increase hydrophobicity. Therefore, if the same soil were used in these experiments, hydrophobicity would remain constant while the PDMS content in the soil increases with wetting–drying cycles.

As for differences between the laboratory-tested soil sample and field natural soils, soils with finer particle sizes, such as silt and clay, may require a higher amount of hydrophobic cargo to induce soil hydrophobicity. Additionally, the presence of organic matter, residual water, and other non-mineral matter can potentially hinder the effectiveness of the treatment [39]. As a result, the application of microcapsules in natural soils, characterized by diverse particle sizes and mineral compositions, requires additional investigation.

Moreover, future work should also consider the release of cargo from microcapsules in solutions, i.e., in a water saturated phase, as this study concerned the release of microcapsules under a drying path and, the influence of

environmental factors such as temperature and pH on the performance of the microcapsules. As an organic material, the calcium alginate capsules are likely to degrade and empty their cargo over time. To minimize such effects, capsules could be deployed when needed through infiltrating solutions. Future studies could also test capsules with a longer durability. For example, capsules produced by in-situ polymerization, have an urea formaldehyde shell with a lifespan in excess of 32 years [41]. However, their environmental impact will need to be accounted for.

4 Conclusions

This study demonstrates the feasibility of encapsulating hydrophobic compounds in calcium alginate microcapsules and subsequent release in fine sands to induce hydrophobicity. Polydimethylsiloxane was encapsulated in calcium alginate microcapsules by the ionic gelation method and subjected to continuous drying and wetting–drying cycles. During drying, the polydimethylsiloxane release increases with time. Under wetting–drying cycles, the release ability of polydimethylsiloxane reduces with the cycles. The polydimethylsiloxane loading (ratio of polydimethylsiloxane to water mass inside the microcapsules) and the microcapsules density (percentage of microcapsules mixed with soil) affected its hydrophobicity enhancement. In general, higher polydimethylsiloxane loading results in a higher sand hydrophobicity and higher microcapsules density results in a higher amount of released PDMS. However, for higher microcapsules density, hydrophobicity decreases due to the higher sand moisture content. Based on the results, 20 PDMS loading and 8% capsule density represents the optimal conditions to deploy microcapsules in infrastructure, since a higher loading increases hydrophobicity while a lower capsules density limits the increase in soil moisture.

Acknowledgements This work was supported by a Collaborative Research Fund from the Research Grants Council Hong Kong (C6006-20GF), a seed funding grant from The University of Hong Kong (201910159115) and Royal Society International Exchanges 2020 R3 (IES\R3\203024).

Data availability The authors confirm that the data supporting the findings of this study is available within the article. The raw/processed data required to reproduce these findings cannot be shared at this time due to technical or time limitations.

References

1. Arora S, Lal S, Kumar S, Kumar M, Kumar M (2011) Comparative degradation kinetic studies of three biopolymers: chitin, chitosan and cellulose. Arch Appl Sci Res 3(3):188–201
2. Augst AD, Kong HJ, Mooney DJ (2006) Alginate hydrogels as biomaterials. Macromol Biosci 6(8):623–633
3. Bachmann J, Horton R, Van Der Ploeg RR, Woche S (2000) Modified sessile drop method for assessing initial soil–water contact angle of sandy soil. Soil Sci Soc Am J 64(2):564–567
4. Bannikova A, Evteev A, Pankin K, Evdokimov I, Kasapis S (2018) Microencapsulation of fish oil with alginate: in-vitro evaluation and controlled release. LWT 90:310–315
5. Bao S, Liu Q, Li H, Zhang L, Maria Barbieri D (2021) Investigation of the release and self-healing properties of calcium alginate capsules in asphalt concrete under cyclic compression loading. J Mater Civ Eng 33(1):04020401
6. Bardet JP, Jesmani M, Jabbari N (2014) Permeability and compressibility of wax-coated sands. Géotechnique 64(5):341–350
7. Bekas DG, Tsirka K, Baltzis D, Paipetis AS (2016) Self-healing materials: a review of advances in materials, evaluation, characterization and monitoring techniques. Compos B Eng 87:92–119
8. Bhandari BR, Patel KC, Chen XD (2008) Spray drying of food materials-process and product characteristics. Dry Technol Food Process 4:113–157
9. Blaiszik BJ, Kramer SL, Olugebefola SC, Moore JS, Sottos NR, White SR (2010) Self-healing polymers and composites. Annu Rev Mater Res 40:179–211
10. Butstraen C, Salaün F (2014) Preparation of microcapsules by complex coacervation of gum Arabic and chitosan. Carbohyd Polym 99:608–616
11. Cao B, Souza L, Xu J, Mao W, Wang F, Al-Tabbaa A (2021) Soil mix cutoff wall materials with microcapsule-based self-Healing grout. J Geotech Geoenviron Eng 147(11):04021124
12. Cesari A, Loureiro MV, Vale M, Yslas EI, Dardanelli M, Marques AC (2020) Polycaprolactone microcapsules containing citric acid and naringin for plant growth and sustainable agriculture: physico-chemical properties and release behavior. Sci Total Environ 703:135548
13. Chan ES, Lee BB, Ravindra P, Poncelet D (2009) Prediction models for shape and size of ca-alginate macrobeads produced through extrusion–dripping method. J Colloid Interface Sci 338(1):63–72
14. Chan LW, Lee HY, Heng PWS (2002) Production of alginate microspheres by internal gelation using an emulsification method. Int J Pharm 242(1–2):259–262
15. Chen K, Qi R, Xing X, Sufian A, Lourenço SD (2023) Constriction size retention criterion for calcium alginate microcapsules in granular materials. Powder Technol 413:118034
16. Chow TT, Long H, Mok HY, Li KW (2011) Estimation of soil temperature profile in Hong Kong from climatic variables. Energy Build 43(12):3568–3575
17. Davidson D, Gu FX (2012) Materials for sustained and controlled release of nutrients and molecules to support plant growth. J Agric Food Chem 60(4):870–876

18. De Koster SAL, Mors RM, Nugteren HW, Jonkers HM, Meesters GMH, Van Ommen JR (2015) Geopolymer coating of bacteria-containing granules for use in self-healing concrete. Procedia Eng 102:475–484
19. Desai KGH, Jin Park H (2005) Recent developments in microencapsulation of food ingredients. Dry Technol 23(7):1361–1394
20. Dong B, Fang G, Ding W, Liu Y, Zhang J, Han N, Xing F (2016) Self-healing features in cementitious material with urea–formaldehyde/epoxy microcapsules. Constr Build Mater 106:608–617
21. Dong Y, Pamukcu S (2020) Synthesis of surface-modified sands with thermoresponsive wettability. J Mater Civ Eng 32(9):04020271
22. Dong Y, Pamukcu S (2015) Thermal and electrical conduction in unsaturated sand controlled by surface wettability. Acta Geotech 10:821–829
23. Gan SN, Shahabudin N (2019) Applications of microcapsules in self-healing polymeric materials. In: Microencapsulation-processes, Technologies and Industrial Applications. IntechOpen.
24. Gharsallaoui A, Roudaut G, Chambin O, Voilley A, Saurel R (2007) Applications of spray-drying in microencapsulation of food ingredients: an overview. Food Res Int 40(9):1107–1121
25. Goebel MO, Bachmann J, Reichstein M, Janssens IA, Guggenberger G (2011) Soil water repellency and its implications for organic matter decomposition—is there a link to extreme climatic events? Glob Change Biol 17(8):2640–2656
26. Gorbunova N, Evteev A, Evdokimov I, Bannikova A (2016) Kinetics of ascorbic acid transport from alginate beads during in vitro digestion. J Food Nutr Res 55(2):148–158
27. Huang G, Lin H, Li J, Liu J (2023) Inducing hydrophobicity in saline soils: A comparison of hydrophobic agents and mechanisms. Powder Technol 424:118475. https://doi.org/10.1016/j.powtec.2023.118475
28. Johnson LM, Gao L, Shields CW IV, Smith M, Efimenko K, Cushing K, Genzer J, López GP (2013) Elastomeric microparticles for acoustic mediated bioseparations. J Nanobiotechnol 11(1):1–8
29. Johnston P, Freischmidt G, Easton CD, Greaves M, Casey PS, Bristow KL, Gunatillake PA, Adhikari R (2017) Hydrophobic-hydrophilic surface switching properties of nonchain extended poly (urethane) s for use in agriculture to minimize soil water evaporation and permit water infiltration. J Appl Polym Sci 134(45):44756
30. Kanellopoulos A, Giannaros P, Al-Tabbaa A (2016) The effect of varying volume fraction of microcapsules on fresh, mechanical and self-healing properties of mortars. Constr Build Mater 122:577–593
31. Kanellopoulos A, Giannaros P, Palmer D, Kerr A, Al-Tabbaa A (2017) Polymeric microcapsules with switchable mechanical properties for self-healing concrete: synthesis, characterization and proof of concept. Smart Mater Struct 26(4):045025
32. Leelamanie DAL, Karube J (2009) Time dependence of contact angle and its relation to repellency persistence in hydrophobized sand. Soil Science and Plant Nutrition 55(4):457–461
33. Letey J, Carrillo MLK, Pang XP (2000) Approaches to characterize the degree of water repellency. J Hydrol 231:61–65
34. Lin H, Lourenco SD (2020) Physical degradation of hydrophobized sands. Powder Technol 367:740–750
35. Lin H, Lourenço SD (2022) Accelerated weathering of hydrophobized sands. Acta Geotech 17(2):377–390
36. Lin H, Lourenço SD, Yao T, Zhou Z, Yeung AT, Hallett PD, Paton GI, Shih K, Hau BC, Cheuk J (2019) Imparting water repellency in completely decomposed granite with Tung oil. J Clean Prod 230:1316–1328
37. Lupo B, Maestro A, Gutiérrez JM, González C (2015) Characterization of alginate beads with encapsulated cocoa extract to prepare functional food: comparison of two gelation mechanisms. Food Hydrocolloids 49:25–34
38. Morris ER, Rees DA, Thom D, Boyd J (1978) Chiroptical and stoichiometric evidence of a specific, primary dimerisation process in alginate gelation. Carbohydr Res 66(1):145–154
39. Ng S, Lourenço S (2016) Conditions to induce water repellency in soils with dimethyldichlorosilane. Géotechnique 66(5):441–444
40. Ni L, Jie X, Wang P, Li S, Hu S, Li Y, Li Y, Acharya K (2015) Characterization of unsaturated fatty acid sustained-release microspheres for long-term algal inhibition. Chemosphere 120:383–390
41. Otake Y, Kobayashi T, Asabe H, Murakami N, Ono K (1995) Biodegradation of low-density polyethylene, polystyrene, polyvinyl chloride, and urea formaldehyde resin buried under soil for over 32 years. J Appl Polym Sci 56(13):1789–1796
42. Polk A, Amsden B, De Yao K, Peng T, Goosen MFA (1994) Controlled release of albumin from chitosan-alginate microcapsules. J Pharm Sci 83(2):178–185
43. Ruiz-Riancho N, Garcia A, Grossegger D, Saadoon T, Hudson-Griffiths R (2021) Properties of Ca-alginate capsules to maximize asphalt self-healing properties. Constr Build Mater 284:122728
44. Samadzadeh M, Boura SH, Peikari M, Kasiriha SM, Ashrafi A (2010) A review on self-healing coatings based on micro/nanocapsules. Prog Org Coat 68(3):159–164
45. Saulick Y, Lourenço S, Baudet B (2016) Effect of particle size on the measurement of the apparent contact angle in sand of varying wettability under air-dried conditions. In: E3S web of conferences, vol 9, p 09003
46. Sethy NK, Arif Z, Mishra PK, Kumar P (2019) Synthesis of SiO_2 nanoparticle from bamboo leaf and its incorporation in PDMS membrane to enhance its separation properties. J Polym Eng 39(7):679–687
47. Singh MN, Hemant KSY, Ram M, Shivakumar HG (2010) Microencapsulation: a promising technique for controlled drug delivery. Res Pharm Sci 5(2):65
48. Talukdar S, Banthia N, Grace JR (2012) Carbonation in concrete infrastructure in the context of global climate change—part 1: experimental results and model development. Cement Concr Compos 34(8):924–930
49. Timilsena YP, Akanbi TO, Khalid N, Adhikari B, Barrow CJ (2019) Complex coacervation: principles, mechanisms and applications in microencapsulation. Int J Biol Macromol 121:1276–1286
50. Vinceković M, Jalšenjak N, Topolovec-Pintarić S, Đermić E, Bujan M, Jurić S (2016) Encapsulation of biological and chemical agents for plant nutrition and protection: chitosan/alginate microcapsules loaded with copper cations and Trichoderma viride. J Agric Food Chem 64(43):8073–8083
51. Wan P, Liu Q, Wu S, Zhao Z, Chen S, Zou Y, Rao W, Yu X (2021) A novel microwave induced oil release pattern of calcium alginate/nano-Fe_3O_4 composite capsules for asphalt self-healing. J Clean Prod 297:126721
52. Wang JY, Soens H, Verstraete W, De Belie N (2014) Self-healing concrete by use of microencapsulated bacterial spores. Cem Concr Res 56:139–152
53. Wang J, Mignon A, Snoeck D, Wiktor V, Van Vliergerghe S, Boon N, De Belie N (2015) Application of modified-alginate

encapsulated carbonate producing bacteria in concrete: a promising strategy for crack self-healing. Front Microbiol 6:1088
54. Wang X, Sun P, Han N, Xing F (2017) Experimental study on mechanical properties and porosity of organic microcapsules based self-healing cementitious composite. Materials 10(1):20
55. Xu D, Chen W, Fan X (2020) Experimental investigation of particle size effect on the self-healing performance of microcapsule for cemented coral sand. Constr Build Mater 256:119343
56. Zhang H, Cheng J, Ao Q (2021) Preparation of alginate-based biomaterials and their applications in biomedicine. Mar Drugs 19(5):264
57. Zheng S, Xing X, Lourenço SD, Cleall PJ (2019) Cover systems with synthetic water-repellent soils. Vadose Zone J 20(1):e20093
58. Zhu DY, Rong MZ, Zhang MQ (2015) Self-healing polymeric materials based on microencapsulated healing agents: From design to preparation. Prog Polym Sci 49:175–220